Journal of Hydrology 561 (2018) 1037–1047

Contents lists available at ScienceDirect

Journal of Hydrology

journal homepage: www.elsevier.com/locate/jhydrol

Research papers

LOMOS-mini: A coupled system quantifying transient water and heat exchanges in streambeds

Karina Cucchi [a,b,*], Agnès Rivière [a], Aurélien Baudin [a], Asma Berrhouma [a], Véronique Durand [c], Fayçal Rejiba [d], Yoram Rubin [b], Nicolas Flipo [a]

[a] Geosciences Department, Mines ParisTech, PSL Research University, Paris, France
[b] Department of Civil and Environmental Engineering, University of California Berkeley, CA, USA
[c] Laboratoire GEOPS, Univ. Paris-Sud, CNRS, UMR 8148 Bât. 504, 91405 Orsay Cedex, France
[d] Sorbonne Universités – UPMC Univ Paris 06, CNRS, UMR 7619 METIS, Paris, France

ARTICLE INFO

Article history:
Received 12 June 2017
Received in revised form 18 September 2017
Accepted 29 October 2017
Available online 31 October 2017
This manuscript was handled by Corrado Corradini, Editor-in-Chief, with the assistance of Subashisa Dutta, Associate Editor

Keywords:
Groundwater-surface water interactions
Hyporheic zone
Experimental methods
Low-cost
Temperature/pressure sensors
In situ measurements

ABSTRACT

The LOMOS-mini is a new experimental system monitoring transient water and heat fluxes in the hyporheic zone at a sub-daily resolution. Given the coupling of high-frequency hydraulic head gradient and temperature measurements, its innovation when compared to currently available monitoring systems is to operate under transient conditions and to allow the quantification of coupled water and heat exchanges with an unprecented fine temporal resolution, such as the rainfall event time scale. The LOMOS-mini is low-cost, easy to construct from individual microelectronic components and has an autonomy of several months in the field. Its robust implementation protocol makes it suitable for a wide variety of geological environments, from soft loamy, sandy, clayey streambeds to compact colluvial environments. Hydraulic head gradients are measured using the pressure sensor technology presented in Greswell et al. (2009). The sensibility of pressure estimates to ambient temperature is demonstrated; the measurement error is evaluated to decrease by up to one order of magnitude when accounting for temperature in the calibration relationship. Coupled with a physically-based hydrothermal model, the LOMOS-mini provides transient estimates of vertically distributed Darcy fluxes, conductive and advective heat fluxes. The methodology is illustrated on a colluvial streambed case study.

1. Introduction

Water and heat exchanges between a stream and its underlying aquifer are critical for water quality and ecosystem health (Boulton et al., 1998; Krause et al., 2011). The mixing zone between surface and subsurface water bodies, known as the hyporheic zone, exhibits unique physical and chemical properties supporting processes essential for the biogeochemical and ecological functioning of river corridors (Boano et al., 2014; Flipo et al., 2014). In particular, water and heat exchanges in the hyporheic zone determine the fate of contaminants in the river-aquifer continuum, the transport of nutrients along the hyporheic corridor and the formation of thermal refugia that provide habitat for river ecosystems (Stanford and Ward, 1988; Malcolm et al., 2005).

Understanding physical, chemical and ecological processes in the hyporheic zone requires a sound hydrogeological description of water exchanges and heat governing these processes (Bencala, 2000; Sophocleous, 2002). Recent years have seen the development of a variety of experimental methods for that purpose (e.g. Kalbus et al., 2006; Rosenberry et al., 2008; Mouhri et al., 2013); these methods are developed to be accurate and reliable, but also low-cost, easy and fast to deploy in the field under the limited time and financial constraints that are always associated with field investigations (Wickert, 2014). Rosenberry (2008) introduced seepage meters providing direct measurements of exchanges across the stream-aquifer interface, but noted that the meters disturb the river flow field and alter measured exchanges, particularly at low flow. Solder et al. (2016) introduced a tube seepage meter allowing for estimates of vertical seepage rates and streambed hydraulic conductivity with minimal perturbation to sediment and water flow. However, it is based on an active change of water levels and therefore provides a snapshot estimate at the time when measurements are taken.

* Corresponding author at: Geosciences Department, Mines ParisTech, PSL Research University, Paris, France.
E-mail addresses: karina.cucchi@mines-paristech.fr, karina.cucchi@berkeley.edu (K. Cucchi).

https://doi.org/10.1016/j.jhydrol.2017.10.074
0022-1694/

The tracking of natural tracers provides valuable information about the magnitude of stream-aquifer exchanges (Xie et al., 2016). In particular, the usage of heat as a tracer of flow in the hyporheic zone has received considerable attention because it is relatively easy, fast and inexpensive to measure (Anderson, 2005; Constantz, 2008). A popular method consists of placing temperature sensors at different depths along a vertical profile in sediments below the stream. The propagation of diurnal temperature variations with depth informs about the magnitude of water exchanges between the stream and the underlying hyporheic zone, using either an analytical approximation to the heat equation with constant seepage and sinusoidal temperature boundary conditions (e.g. Hatch et al., 2006; Keery et al., 2007; Cuthbert et al., 2010), or with the help of a numerical model solving for transient flow and heat transport along a vertical sediment column (e.g. Anibas et al., 2009; Cranswick et al., 2014). Recent analytical development by Caissie and Luce (2017) permit to estimate transient conductive and advective fluxes driven by diurnal and annual temperature variations from vertically-distributed temperature time series, but still relying on constant seepage velocity calibrated from a numerical model.

This paper presents a new sampling system called LOMOS-mini (LOcal MOnitoring Station-mini), which monitors vertical water and heat exchanges between a stream and its underlying aquifer at higher temporal frequency than other currently existing methods. The LOMOS-mini relies on the coupling of pressure and temperature measurements. The main benefit of the LOMOS-mini is the quantification of water and heat exchanges at a sub-daily resolution (e.g. every 15 min) when used in combination with a vertically distributed hydrothermal numerical model. In particular, temporally-varying response to particular hydrological events can be quantified (Rosenberry et al., 2013). For example, Dudley-Southern and Binley (2015) showed that the rapid rise of surface water levels after a rainfall event can lead to a temporary reversal of flow direction towards infiltration in the hyporheic zone. Monitoring methods available to date do not allow for the quantification of this reversal in water fluxes and associated heat fluxes at a sub-daily resolution.

The main objective of this paper is to introduce the LOMOS-mini, designed to be easy to use, inexpensive and reliable in the field. The design of the pressure and temperature sensors and their implementation on the field are described, and the use of a LOMOS-mini is illustrated with a set of experimental measurements and corresponding flux estimates. The deployment of several LOMOS-mini will provide the ability to monitor water and heat fluxes between a stream and its underlying aquifer at high spatial and temporal resolution.

This paper is organized as follows. The first part presents the sampling system. The second part is dedicated to the calibration procedure, particularly demonstrating the necessity of taking into account the effect of temperature when deriving hydraulic head gradients. The last part describes the implementation of LOMOS-mini in the field and illustrates its ability to monitor high-frequency stream-aquifer exchanges on a case study in the Avenelles basin, France (Mouhri et al., 2013), where the streambed is composed of loess and underlaid by colluvium with blocks of gritstone, a rarely sampled type of hyporheic zone.

2. Presentation of the LOMOS-mini

The LOMOS-mini draws from LOMOS stations presented in Mouhri et al. (2013) for monitoring spatially-distributed and temporally-varying stream-aquifer exchanges. In both cases, the quantification relies on a combination of hydraulic head differential and temperature measurements. Mouhri et al. (2013) applied their methodology to a small sedimentary basin, the Avenelles basin, France. Five LOMOS stations placed along the hydrological network monitored the stream-aquifer exchange dynamics from hydraulic head and temperature measurements. Each LOMOS station consists of piezometers located in both banks of the stream, and of a pressure sensor located in the stream and monitoring the stream stage. All sensors also monitor temperature and constrain the boundaries of a two-dimensional stream cross-section. Heat is then used as a tracer of the flow to estimate continuous records of stream-aquifer exchanges.

Similar to the LOMOS, the LOMOS-mini couples hydraulic head gradient measurements with temperature measurements. Whereas the LOMOS constrains flow within a stream cross-section, LOMOS-mini measurements are taken along a vertical column within the hyporheic zone at the local scale (~0.1–1 m) (Flipo et al., 2014). This redesign implies to modify the monitoring system, so that (1) it operates within the streambed instead of the stream banks and (2) it is able to measure hydraulic head differentials of the order of a few centimeters or less. This is the role of the pressure differential sensor presented in Section 3. The one-dimensional (1D) column along which measurements are taken is typically 40–80 cm deep, although it can be easily adjusted depending on characterization needs. Fig. 1 presents the monitoring system along a vertical cross-section for the infiltrating case, where hydraulic head is higher in the stream than at the bottom of the hyporheic zone, and flow is directed downwards.

The LOMOS-mini is designed to be installed in low-order streams, with a typical Strahler number of 1–3 (Strahler, 1952), and is thus adapted to monitor upstream river networks where discharge genesis usually occurs. The streams need to be accessible by foot, and it is recommended to make the installation when the water level in the stream is lower than 1 m to ensure that the implementation of the device in the streambed is possible. The LOMOS-mini is designed to operate under saturated conditions (Section 4.1), where the river and the hyporheic zone are connected (Brunner et al., 2009). The LOMOS-mini is a low-cost system, which can be constructed for about 500€including the two Onset® Hobo® data loggers. As further detailed in Section 4.1, the implementation of the LOMOS-mini is robust and therefore suitable for a variety of geological environments with different compactness, from soft porous media such as sandy streambeds to more compact porous media such as colluvial streambeds.

The first part of the LOMOS-mini is the temperature system (Fig. 1a). Temperature time series are measured in the stream and at several depths along a vertical profile in the hyporheic zone. Temperature sensors are typically installed along a stick at depths of 10, 20, 30 and 40 cm below the streambed, although the depth and the spacing between probes is adjustable. They monitor the propagation of temperature variations with depth with a typical sampling period of 15 min. The in situ implementation of the temperature system is detailed in Section 4.1.

The second part is the monitoring of hydraulic head gradient between the surface and the hyporheic zone (Fig. 1b). A pressure differential sensor is installed in the direct vicinity of the temperature system and measures the differential in hydraulic head between the streambed and the bottom of the 1D column. The pressure sensor samples every fifteen minutes synchronously with the temperature measurements. The mechanical and electronic functioning of the pressure sensor is detailed in Section 3.

To the authors' knowledge, the LOMOS-mini is the first system monitoring coupled water and heat exchanges at a high frequency (e.g. 15 min), and can therefore provide critical insight for better understanding hydrological, geochemical and ecological processes in the hyporheic zone. The potential offered by the LOMOS-mini for quantifying stream-aquifer exchanges at high-frequency is further illustrated in Section 4.3.

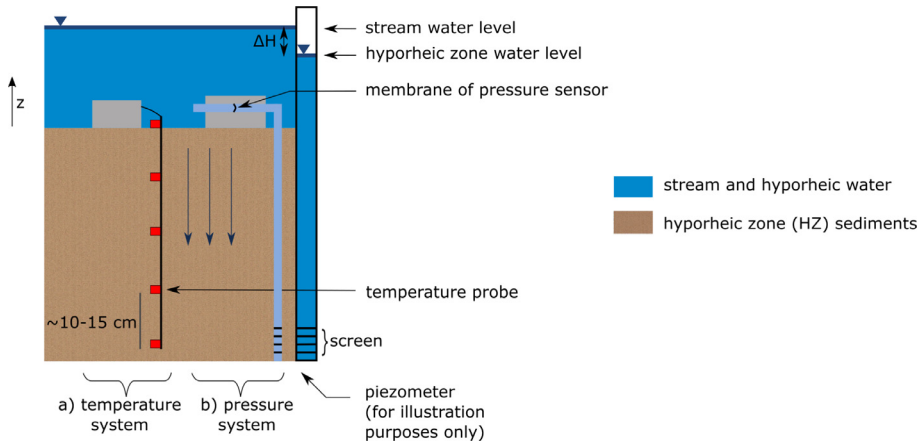

Fig. 1. Schematic view of the LOMOS-mini along a vertical cross-section. The technology relies on the coupling of (a) vertically-distributed temperature time series measurements and (b) hydraulic head differential between the stream and the underlying hyporheic zone. The membrane deformation allows to measure the evolution of the hydraulic head differential ΔH in time. The piezometer in the right hand side of the Figure is presented for a better conceptual understanding and is not physically present in the field.

3. The pressure sensor

This section presents the pressure part of the LOMOS-mini system, which monitors the difference in hydraulic head between the top and the bottom of the vertical sediment column. These measurements of typically a few centimeters or less are challenging to obtain with sufficient accuracy (Essaid et al., 2008). The functioning of the pressure sensor is presented and the experimental steps for its calibration accounting for sensitivity to temperature are described.

3.1. Mechanical and electronic functioning of the pressure sensor

The pressure sensor is built upon the technology presented in Greswell et al. (2009), modified by implementing an adjustable gain in the electronic circuit to better target ranges of hydraulic head differential observable between the stream and the hyporheic zone (as detailed further in the section). The main points of the electronic implementation are repeated here.

The hydraulic head differential monitoring relies on a pressure transducer converting the water pressure differential between the stream and the hyporheic zone into an electrical voltage, which is measured by the data logger. Measuring pressure in the form of a differential between the stream and the hyporheic zone avoids the need for barometric pressure compensation. The pressure transducer used in the LOMOS-mini is the 26PCA series pressure sensor designed by Honeywell, USA. This sensor contains a piezoresistive membrane bending with an amplitude depending on the pressure differential applied on both sides of the membrane (Fig. 2). Placed between the tube going to the river and the one going to the hyporheic zone, this membrane outputs an electrical voltage proportional to the difference in pressure between the top and the bottom of the sediment column. The 26PCA series sensor monitors pressure differentials with a magnitude of up to 1 psi (0.7 m water head) in both directions, and it resists to pressure differentials of up to 20 psi (14 m), showing robustness to field conditions. The sensor can record both negative and positive pressure differentials and is thus capable of monitoring hydraulic head differentials under both infiltration and exfiltration conditions. The pressure sensor sensitivity is 8.35 mV/psi (0.119 mV/cm head) when powered with 5 V.

A second part in the electronic circuit adjusts the voltage delivered by the piezoresistive membrane to the range made available by the data logger. The data logger is an Onset® Hobo®, and records voltages in the 0–2.5 V range. An analog amplifier with adjustable gain is set such that the LOMOS-mini monitors hydraulic head differential ranging between about +10 and −10 cm; for most sites and most hydraulic conditions, this range in hydraulic head differential is an overestimation of expected hydraulic head differentials between the top and the bottom of a 40 cm hyporheic zone column. Given the pressure sensor sensitivity, the targeted hydraulic head differential range, and the data logger recording range, the gain is set to be on the order of 10^3, amplifying the signal delivered by the piezoresistive membrane from the order of millivolts to the order of volts. Notably, the value chosen for the gain does not impact the final error made with the sensor. Finally, a 1.25 V reference diode is placed in the electronic circuit to shift the final voltage range to 0–2.5 V, as recorded by the Onset® Hobo®.

3.2. Calibration

The pressure logger outputs an electrical voltage, primarily function of the deformation of the membrane under the applied pressure differential. Besides the membrane deformation, the electronic circuit is also very sensitive to temperature fluctuations. The relationship between pressure differential, temperature and voltage depends on the gain chosen for the amplifier, but also on the temperature sensitivity of each individual component in the electronic circuit. Therefore, each pressure system needs to be individually calibrated.

This section describes the experimental protocol for calibrating the pressure sensor; and establishes the final relationship between hydraulic head differential, voltage and temperature from presented calibration experiments.

3.2.1. Establishing the relationship between voltage and hydraulic head differential

First, the calibration of voltage measurements with respect to hydraulic head differential is performed. This calibration is performed at ambient temperature. During the calibration period, temperature is close to constant and automatically monitored at a high frequency (e.g. every 1 min).

A specific design is constructed for the calibration between hydraulic head differential and voltage (Fig. 3a). Two tubes, the left reproducing the river stage H_{riv} and the right reproducing the hyporheic zone hydraulic head H_{HZ}, are placed vertically and are connected to the pressure sensor. The water height in each tube is modified, and the hydraulic head differential and the electrical

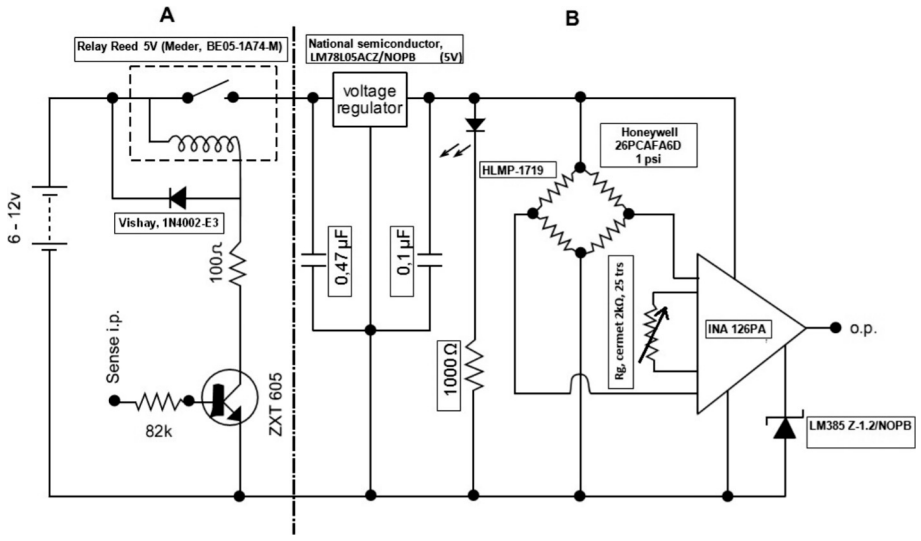

Fig. 2. Diagram of the electronic circuit of the pressure sensor, adapted from Greswell et al. (2009) by implementing an analog amplifier with variable gain.

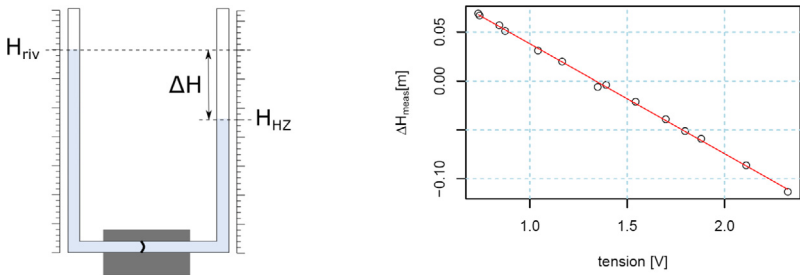

(a) Experimental setup for the calibration of voltage U as a function of head differential ΔH.

(b) Hydraulic head differential ΔH applied to the pressure sensor as a function of the measured voltage U

Fig. 3. Calibration of voltage with respect to hydraulic head differential, at ambient temperature T_{ref}.

voltage measured by the pressure sensor are reported for multiple configurations of water heights H_{riv} and H_{HZ}. The entire range of hydraulic head differential is covered, until reaching the saturation of the data logger, at 0 and 2.5 V (Fig. 3b). The measurements indicate a linear relationship between voltage U and hydraulic head differential $\Delta H, \Delta H = H_{HZ} - H_{riv}$, until saturation of the data logger is reached.

A linear curve is then fitted to measurements not included in the data logger saturation zone. The fitting relationship is presented in Eq. (1), where fitted coefficients α and β are estimated from measurements of the calibration experiment.

$$\Delta H(U, T_{ref}) = \alpha + \beta U \tag{1}$$

3.2.2. Sensitivity to temperature

As mentioned in Greswell et al. (2009), the electrical voltage measured at the output of the pressure sensor is sensitive to the ambient temperature at which measurements are taken. This section presents the calibration method used to quantify the sensitivity of the pressure sensor to temperature conditions.

Experiments used to establish the sensitivity of voltage measurements to temperature variations are conducted in a climatic chamber (Fig. 4a). The climatic chamber is convenient because it enables the control of temperature in the environment where pressure measurements are taken. The behavior of the pressure sensor can be tested in a wide range of temperature settings controlled via a programming interface. A thermostatically-controlled water bath with programmable temperature variations can equivalently be used, when available.

Three separate experiments are conducted for each sensor. In each experiment, a fixed hydraulic head differential is applied to the pressure sensor in the climatic chamber, where temperature is programmed to vary linearly in ranges corresponding to temperature conditions that LOMOS-mini can experience in the field. The voltage and ambient temperature in the climatic chamber are recorded with a one-minute periodicity.

These experiments show that for a fixed hydraulic head differential, the measured difference in electrical potential varies with temperature, in a linear fashion (Fig. 4b). The voltage signal is noisy, this is due to the vibration of the climatic chamber caused by the motor control. Only the linear fit of voltage variations is considered when interpreting the signal.

3.2.3. Establishing the relationship between $\Delta H, U$ and T

Calibration experiments described in Sections 3.2.1 and 3.2.2 allow the quantification of measurement errors when the effect of temperature is not taken into account. The error quantification is achieved by the mean of a calibration relationship between hydraulic head differential ΔH, output voltage U and temperature T. First, coefficients α and β from Eq. (1) are estimated based on

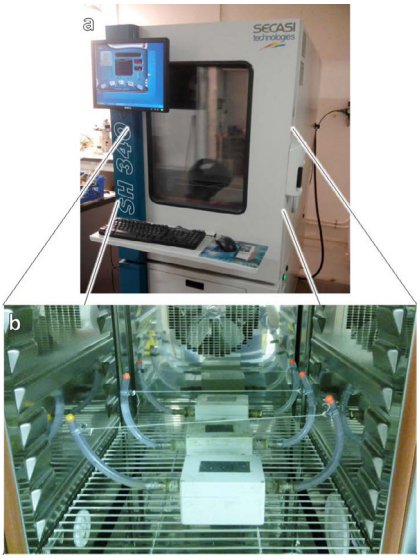

(a) Experimental setup for monitoring the influence of temperature variations on voltage measurements. Tubes on each side of pressure sensor boxes are filled with water corresponding to a hydraulic head differential, this hydraulic head differential remains constant while the temperature in the climatic chamber varies. The voltage is recorded for this constant hydraulic head differential and varying temperature conditions. (a) climatic chamber and programming interface (b) pressure boxes inside the climatic chamber

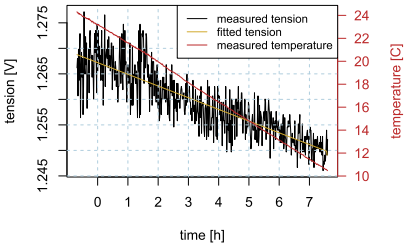

(b) Example of voltage (in black) and temperature (in red) time series measured during the experiment, for a constant hydraulic head differential (here $\Delta H = +2.3cm$). The noise in the measured voltage time series is due to the vibrations caused by the motor control in the climatic chamber.

Fig. 4. Experimental setup and measurements for the calibration of the pressure sensor to temperature variations.

data from experiment 3.2.1. Then, data from experiment 3.2.2 are used to calculate the hydraulic head differential ΔH_{fit} corresponding to the voltage measured in the climatic chamber when using Eq. (1), which does not account for the effect of temperature. Finally, ΔH_{fit} is compared to the hydraulic head differential ΔH_{meas} applied during the experiment in the climatic chamber. The difference between the fitted hydraulic head differential ΔH_{fit} and the hydraulic head differential applied in the climatic chamber ΔH_{meas} informs on the estimation error (Fig. 5a).

The variation of this estimation error with ambient temperature provides the sensitivity of the calibration relationship to ambient temperature. Fig. 5a shows how the error increases as the difference between the ambient temperature and the temperature $T_{ref} = 18\,^{\circ}$C used when establishing the calibration relationship (Eq. (1)) increases. When the ambient temperature is 5 °C, the introduced bias is as high as +2 cm. This justifies the modification of Eq. (1) into Eq. (2) which accounts for temperature.

In order to account for the effect of temperature on the relationship between voltage and hydraulic head differential, the calibration relationship (Eq. (1)) is modified to include the temperature variable (Eq. (2)).

$$\Delta H = \xi_0 + \xi_1 U + \xi_2 T \tag{2}$$

Coefficients ξ_0, ξ_1 and ξ_2 are estimated using data from both experiments. The coefficient ξ_2 accounting for the influence of temperature in the relationship between ΔH and U is estimated by fitting errors as a function of temperature (Fig. 5a). All three coefficients can then be estimated by relating Eqs. (1) and (2), noting that Eq. (1) is Eq. (2) for $T = T_{ref}$.

These treatments are executed in the form of R scripts (R Core Team, 2013), which provide calibration coefficients ξ_i from data provided in experiments 3.2.1 and 3.2.2. Coefficient values obtained during calibrations of five different pressure sensors are summarized in Table 1.

Fig. 5b shows errors in hydraulic head differential estimates as a function of temperature. Residual variability remains in the estimates, due to the imperfection of the technology and measurements, such as the hysteresis of the membrane or the temporal lag between air temperature variations and temperature of water in contact with the membrane.

When temperature is not taken into account in the calibration relationship (i.e. when Eq. (1) is used for calibration), errors associated with temperatures close to 5 °C are on the order of 2 cm. In comparison, when taking into account the effect of temperature on the calibration relationship, errors associated with temperatures close to 5 °C are on the order of 2 mm. Taking into account

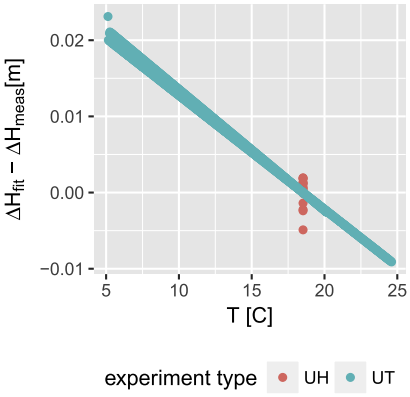

(a) Error for ΔH when temperature is not taken into account in the calibration relationship (Eq. 1), estimated by deriving hydraulic head estimates with Equation 1 from voltage measurements in calibration experiments (ΔH_{fit}), and comparing to the actual hydraulic head differential applied (ΔH_{meas}).

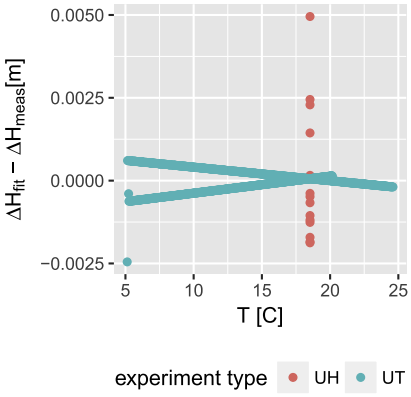

(b) Error for ΔH when temperature is taken into account in the calibration relationship (Eq. 2), estimated by deriving hydraulic head estimates with Equation. 2 from voltage and temperature measurements in calibration experiments (ΔH_{fit}), and comparing to the actual hydraulic head differential applied (ΔH_{meas}).

Fig. 5. Difference between hydraulic head differential imposed in calibration experiments and estimated from calibration relationships (Eqs. (1) and (2)). The dots are colored by experiment type: UH refers to the calibration of voltage with respect to hydraulic head differential (described in Section 3.2.1), UT refers to measurements to the calibration of voltage with respect to temperature (described in Section 3.2.2). Here, the consideration of temperature in the calibration relationship reduces the estimation error from 2 cm to 2 mm.

Table 1
Summary statistics of calibration coefficients in Eq. (2), derived for five pressure sensors.

	ξ_0 [m]	ξ_1 [m/V]	ξ_2 [m/C]
Minimum value	0.179	0.112	0.000451
Median value	0.241	0.183	0.000897
Maximum value	0.827	0.684	0.00154

the temperature correction can therefore reduce the estimation error on ΔH by up to one order of magnitude.

4. Deployment of the LOMOS-mini in the field

This section presents the installation of the LOMOS-mini in the field, emphasizing how the experimental solution proposed is robust, avoiding the contact between the electronic equipment and water and enabling the monitoring in compact geological settings. A set of time series measured in the field is shown, and is used to estimate transient and vertically-distributed water and heat fluxes with the help of a numerical hydrothermal model.

4.1. In situ implementation of the LOMOS-mini

LOMOS-mini measurements rely on the installation of the pressure and temperature systems in close proximity. Fig. 6 shows the final installation of the LOMOS-mini system in the field. This installation takes between 1 and 3 h, depending on the resistance of the streambed sediments to the insertion of the hyporheic tube.

The purpose of the pressure system is to measure the hydraulic head differential between a point at depth in the hyporheic zone and the stream using the electronic circuit presented in Section 3. This circuit is placed at the center of a waterproof box in hydraulic connection to the river and to the hyporheic zone (Figs. 6A, a–c and 6B). The box is designed to contain the equipment supporting the electronic circuit, including a pack of six AA batteries with 1.5 V individual voltage powering the electronic circuit with a voltage greater than 7 V (Fig. 6B, d); and the Hobo device, which serves both as trigger for taking measurements and as data logger (Fig. 6B, f).

Several steps are followed to minimize chances of contact between water and electronic equipment inside the box. First, the electronic circuit implemented on an electronic board is flown into a silicone rubber (Fig. 6B, g). Silicone rubbers are easy to vulcanize and have a wide biological resistance, they are therefore well suited to protect the electronic equipment. Second, all components are placed in a hermetically sealed plastic box; the box follows the IP68 standard, resisting to continuous immersion beyond 1 m (IP6, 2005). A fluoroelastomer at the contact between the lid and the box ensures that the box is hermetically sealed. 4 screws firmly seal the lid to the box. The contact zone between the box and its lid is wrapped in electrical tape as an additional security to water intrusions. Finally, balls of silica gel serve as a desiccant to absorb residual humidity that can appear from condensation. Experience has shown that these steps minimize the risk of water intrusion in the box. Following these steps ensures that electronic components remain dry throughout the in situ experiment, during which the box can be continuously immersed in water for several weeks.

The pressure sensor located inside the pressure box is connected to two tubes, one going to the river and one going into the hyporheic zone. Each tube is made of flexible and transparent plastic with inner diameter 16 mm and outer diameter 20 mm. The stream tube is a few centimeters long and connects the pressure sensor to the pressure in the stream, a fine grid placed at its extremity prevents the intrusion and clogging of elements inside the tube (Fig. 6A, b). The hyporheic tube is positioned in the streambed, its extremity at a depth equal to the depth of the

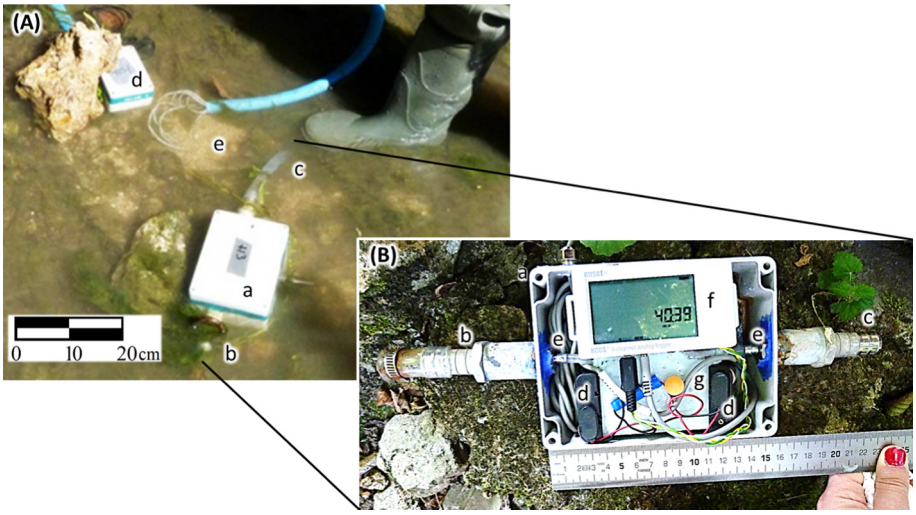

Fig. 6. In situ implementation of the LOMOS-mini in the field. (A) Final implementation. a: pressure sensor box; b: tube to river; c: tube to hyporheic zone; d: temperature box; e: location of temperature sensors at depth in the hyporheic zone. The foot and the scalebar indicate the approximate scale. (B) Inside the pressure box. a: pressure sensor box; b: ribbed connection to river tube; c: ribbed connection to hyporheic tube; d: batteries; e: hydraulic connections from pressure membrane sensor to tubes external to the box; f: data logger; g: silicon rubber surrounding electronic circuit. The ruler provides the scale (in centimeters).

deepest temperature sensor (Fig. 6A, c). The bottom of the tube is perforated along 2–3 cm, so that the hydraulic head in the tube equals the hydraulic head in the hyporheic zone at depth.

Positioning the tube into the hyporheic zone is a delicate step, especially so in compact geological environments such as colluvial environments. It is achieved by pushing the tube with a manual drilling system as follows. First, an aluminum lost tip is fixed to the extremity of the tube. The plastic tube is then inserted inside a more solid metal tube with inner diameter slightly larger than the outer diameter of the hyporheic tube. A clamping ring fixed around the metal tube then allows the use of a hammer to push the hyporheic tube into the subsurface. It is the use of a metal tip and hammer that allows the installation of such systems in compact geological environments. Once the desired depth is reached, the hammer and metal tubes are removed and leaving the hyporheic tube in place. The hyporheic tube is then fixed to the ribbed connection of the pressure box, ensuring no pressure head loss or water intrusion at the connection (Fig. 6B, c).

After the installation, the pressure membrane is at the interface between stream water and hyporheic zone water. The system is designed for saturated hyporheic zones in connection with the stream (Brunner et al., 2009). Indeed, the hydraulic head in the hyporheic zone needs to be greater than the elevation of the pressure sensor to maintain hydraulic connection between the pressure sensor and the water in the hyporheic zone.

The temperature system is implemented in the vicinity of the pressure system (Fig. 6A, d–e). The temperature probes are 3-wires 10 $k\Omega$ NTC sensors compatible with the Hobo data logger (Water/Soil Temperature Sensor TMC6-HD provided by Onset®). The metal cap on the sensor has a cylindrical shape with height 25 mm and diameter 5 mm; therefore the temperature measured at one depth is integrated over the 25 mm of the metal sensor. These probes measure temperature above 0 °C with ±0.3 °C accuracy. Four temperature probes are placed at regular intervals along a plastic sick on which notches of the size of the temperature caps are cut. Plastic is chosen because it is a thermal insulator and it is resistant to field conditions. The insertion of the temperature stick in the hyporheic sediments is done by first drilling a hole using a metal tube ending with a tip. The metal tube is then removed and replaced by the stick where the vertically-distributed temperature probes are fixed. Each temperature sensor is connected to one Hobo slot. The Hobo is then placed in a waterproof box with similar characteristics than the pressure box.

Both the pressure and the temperature boxes need to be waterproof and to resist immersion in the stream over several weeks. Indeed, the challenge in the field is to maintain the hydraulic connection of the circuit to the stream and hyporheic zone waters while keeping the electronic circuit dry in a waterproof environment. Moreover, experience has shown that maintaining the temperature box under water minimizes the risk of seeing wild life damaging electrical cables linking temperature probes to the data logger.

4.2. Measured set of time series in the field

This section presents a set of time series measured for one installation of the LOMOS-mini system in the field. Water and heat exchanges estimated from this set of measurements are presented in Section 4.3.

The LOMOS-mini system was tested at the Avenelles basin, a sedimentary catchment in the Seine basin (Loumagne and Tallec, 2013). The Avenelles basin is a well-instrumented site where the monitoring network has been designed to quantify stream-aquifer exchanges over multiple scales (Mouhri et al., 2013). Measurements presented in this section correspond to the installation of a LOMOS-mini system in the middle part of the Avenelles basin, at a location where the streambed is composed of loess and underlaid by colluvium with blocks of gritstone. To the authors' knowledge, this is one of the first experiments in this type of environment for the quantification of hyporheic exchanges.

Fig. 7 shows temperature and hydraulic head differential time series measured by a LOMOS-mini. Hydraulic head estimates using both calibration relationships are presented, one where temperature is taken into account in the calibration relationship (Eq. (1)), one where temperature is not taken into account (Eq. (2)). It is critical to account for the influence of temperature on hydraulic head differential estimates when investigating hydraulic head differential in the hyporheic zone, where measurements need to be precise in the order of a few millimeters. Discarding the temperature effect when transducing voltage measurements to hydraulic head differential estimates can result in underestimating hydraulic head differential. In some cases, not taking into account the

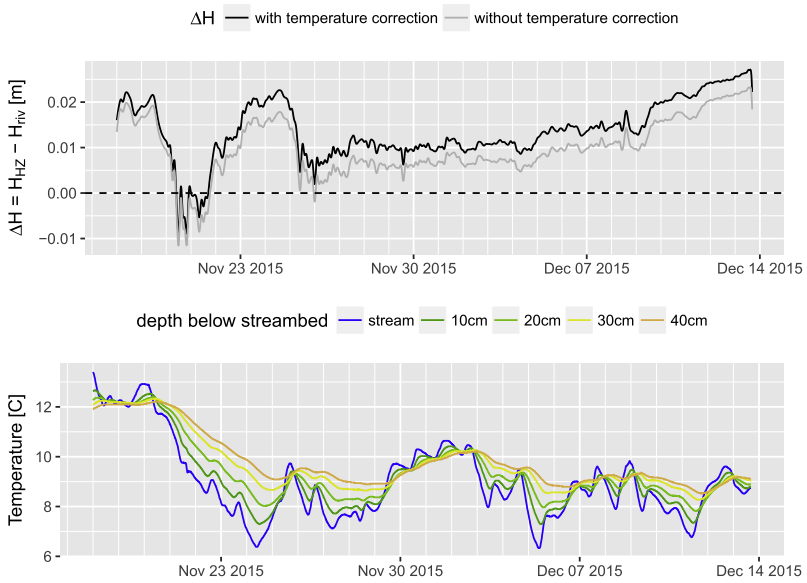

Fig. 7. Set of hydraulic head differential and temperature time series as obtained by a LOMOS-mini system. Discarding the effect of temperature in the calibration relationship results in bias in hydraulic head differential estimates.

temperature effects can also lead to a misconception of the direction of exchanges, for example when head differentials fluctuate around 0 m in Fig. 7.

4.3. Estimating exchanged fluxes from LOMOS-mini measurements

This section presents an example of flux estimates to illustrate the potential of the monitoring system when hydrological and thermal properties in the streambed are known. When properties are unknown, hydrological and thermal parameters can be estimated using inversion methods, this will be the focus of later studies.

Temperature and hydraulic head along the 1D vertical column can be simulated by a transient heat transport and water flow numerical model. This study uses the numerical model Ginette, a fully coupled transient finite volume model solving for water and heat transport in porous media (Rivière et al., 2014). Boundary conditions applied to the numerical model are the hydraulic head differential time series, as well as the top and bottom temperature time series. The other temperature time series can be used to validate the choice of hydrological and thermal parameters in the numerical simulation. Simulated temperature and hydraulic head time series are sensitive to the initial temperature and pressure field assigned to the 1D column, therefore a spin-up period of 2 days is discarded from the analysis. Hypotheses associated with this approach are that water and heat fluxes between the stream and the aquifer are vertical, that spatial variability of water and heat fluxes in the spacing between the pressure and the temperature probes is neglectable, and that hydrological and thermal properties in the sediment column are known.

Fig. 8 shows vertical water and heat exchanges estimated from the set of measurements presented in Fig. 7. Soil properties used in the numerical simulation are summarized in Table 2. The corresponding root mean squared error between measured and simulated temperature time series is 0.05 °C. Fluxes are extracted from the numerical model at the top cell, they therefore represent the conditions right at the interface between the stream and the hyporheic zone. In Fig. 8, colored time periods correspond to a positive thermal gradient in the column, when temperature in the stream is higher than temperature at the bottom of the sediment column and when the stream is therefore expected to lose heat by thermal conduction. These time periods are derived from the measured temperature time series presented in Fig. 7.

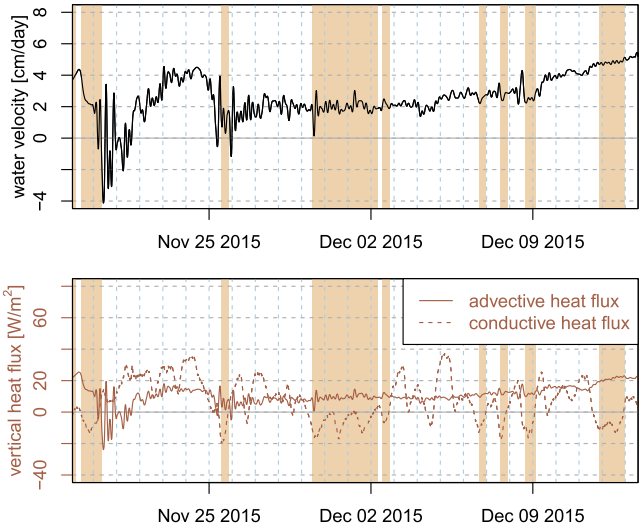

Fig. 8. Time series of vertical water and heat exchanges estimated from the LOMOS-mini set of measurements presented in Fig. 7 using the numerical model Ginette (Rivière et al., 2014). Fluxes are positive upwards. Colored time periods correspond to positive thermal gradients in the column, when temperature is higher in the stream than at the bottom of the hyporheic zone. (For interpretation of the references to color in this figure legend, the reader is referred to the web version of this article.)

Table 2
Values of hyporheic zone properties used in the numerical simulation.

Soil property	Numerical value	Unit
Intrinsic permeability	$9.17 \cdot 10^{-13}$	m^2
Porosity	0.15	–
Solid thermal conductivity	3.38	$kg \cdot m \cdot s^{-3} \cdot C^{-1}$
Solid thermal capacity	10^4	$m^2 \cdot s^{-2} \cdot C^{-1}$
Specific density	$2.5 \cdot 10^3$	$kg \cdot m^{-3}$

The use of a transient model provides a detailed description of dynamics of the water and heat fluxes. At the location and period

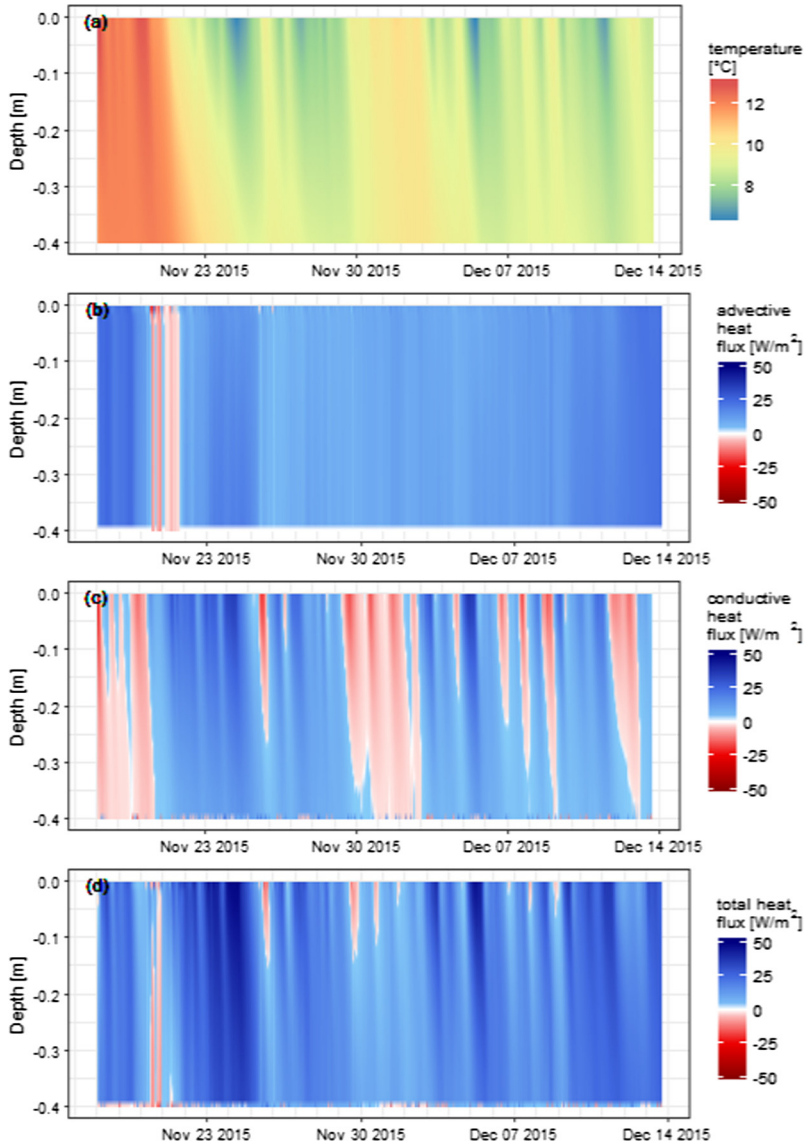

Fig. 9. Temporal estimation of vertically-distributed (a) temperature, (b) advective heat flux, (c) conductive heat flux and (d) total heat flux from the LOMOS-mini set of measurements presented in Fig. 7 with the numerical model Ginette (Rivière et al., 2014). Fluxes are positive upwards.

associated with measurements, water velocity was mostly positive, corresponding to a gaining stream where water flows from the hyporheic zone into the stream (Fig. 8). This is in line with the positive head differential along the 1D column observed in Fig. 7, where the hydraulic head is higher at the bottom of the hyporheic zone than at the top during most of the recording. A gain of thermal energy in the stream by advection are expected during time periods when water velocity is positive.

Fig. 8 shows that the direction of advective heat fluxes is closely related to the magnitude of the water fluxes, as expected. Conductive heat flux shows a higher temporal variability, with a daily periodicity due to diurnal variations of stream temperature. During the day, when stream temperature is higher than hyporheic zone temperature, the conductive heat flux is lower than average, this corresponds to a situation where the heat propagates towards the hyporheic zone. On the contrary, during the night, when stream temperature is lower than hyporheic zone temperature, the conductive heat flux is higher than average. Another noticable point is the correspondance between the direction of the conductive flux and the sign of the thermal gradient in the hyporheic column. As expected, when the thermal gradient is positive (i.e. when temperature is higher in the stream than at the bottom of the hyporheic zone), the conductive heat flux is negative (i.e. hyporheic zone sediments conduct heat downwards).

Fig. 9 further illustrates the potential of measurements taken by the LOMOS-mini system by showing the spatial distribution of temperature and heat fluxes along the vertical column in the hyporheic zone. Fig. 9a shows the temperature profiles along the 1D column and the well-documented propagation and dampening of the diurnal temperature variations with depth. Advective fluxes (Fig. 9b) are homogeneous along the 1D column, this is because they are proportional to the water velocity which is homogeneous along the 1D column. Conductive fluxes exhibit a higher spatial variability (Fig. 9c). Frequent reversals in the direction of conductive fluxes at the top of the column are due to the propagation of stream diurnal temperature fluctuations in the porous media. The depth of this reversal varies from day to day, as the magnitude of daily temperature variations in the stream varies.

Figs. 8 and 9 illustrate the importance of the conductive term when quantifying heat exchange in the hyporheic zone, however

noting that even for low Darcy velocity, the advective term has the same order of magnitude than conductive heat flux.

Coupled with a numerical model, a LOMOS-mini therefore enables high-frequency estimation of advective and conductive heat fluxes along a vertical streambed profile. As illustrated in Fig. 9b,c,d, under stable hydraulics conditions, most heat fluxes reversals are due to diurnal stream temperature fluctuations, while the advective terms become predominant under transient hydrological conditions, then driving energy flux reversals.

5. Conclusion

This paper introduces the LOMOS-mini, an innovative experimental sensor monitoring water and heat exchanges in the hyporheic zone at a sub-daily temporal resolution (e.g. every 15 min). The sensor operates under saturated conditions and monitors vertical exchanges at the local scale (~0.1–1 m). When compared to other available methods, LOMOS-mini measurements allow to relax the assumption of steady water flux, and therefore enable the quantification of transient water exchanges accounting for dynamic hydrologic boundary conditions.

The LOMOS-mini has been used intensely in the field and has proven to be resistant to a variety of climatic and hydrological conditions. Building upon the pressure sensor technology presented by Greswell et al. (2009), the LOMOS-mini coupled pressure and temperature sensor pursues a similar purpose in that it is an easy-to-use, inexpensive and robust equipment for automated data collection in the field. It is therefore well suited for researchers and practitioners usually operating under time constraints and on a limited budget.

Stream-aquifer exchanges result from a variety of hydrological and geomorphological controls, characterized by low and high temporal frequencies as well as spatial heterogeneity; they therefore exhibit high variability over multiple temporal and spatial scales (e.g. Flipo et al., 2014). The LOMOS-mini offers a novel insight into the temporal complexity of local vertical exchanges by enabling the quantification of fluxes driven by dynamic hydrological boundary conditions, which can have the same order of magnitude than those driven by the well-studied stream geomorphologic features (Schmadel et al., 2016). Moreover, the LOMOS-mini is designed to be easy to deploy in the field, and when installed at multiple locations LOMOS-mini sensors can provide spatially-distributed information on the exchange dynamics. For these reasons, the LOMOS-mini is expected to contribute to future efforts supported by field data aiming at upscaling hyporheic exchanges, measurable at the local scale, to the reach and catchment scales.

Acknowledgements

This material is based upon research supported by the PIREN-Seine, the project Traversière of the French Institute Carnot M.I.N.E.S., the Chateaubriand Fellowship of the Office for Science & Technology of the Embassy of France in the United States, and the Jane Lewis fellowship from the University of California, Berkeley. The authors thank Dr. Christelle Courbet from IRSN for funding the construction of the first LOMOS-mini prototype, as well as Noelia Carrillo and Edmée Cuisinier for their contributions to experiments. They acknowledge the efforts of Dr. Heather Savoy and Dr. Bradley Harken for proof-reading the manuscript. Finally, they thank the anonymous reviewers for their detailed suggestions which helped improve the quality of the manuscript.

References

Anderson, M.P., 2005. Heat as a ground water tracer. Groundwater 43 (6), 951–968. https://doi.org/10.1111/j.1745-6584.2005.00052.x.

Anibas, C., Fleckenstein, J.H., Volze, N., Buis, K., Verhoeven, R., Meire, P., Batelaan, O., 2009. Transient or steady-state? Using vertical temperature profiles to quantify groundwater-surface water exchange. Hydrol. Processes 23, 2165–2177. https://doi.org/10.1002/hyp.7289.

Bencala, K.E., 2000. Hyporheic zone hydrological processes. Hydrol. Processes 14 (15), 2797–2798. https://doi.org/10.1002/1099-1085(20001030)14:152797::AID-HYP4023.0.CO;2-6.

Boano, F., Harvey, J.W., Marion, A., Packman, A., Revelli, R., Ridolfi, L., Wörman, A., 2014. Hyporheic flow and transport processes: mechanisms, models, and biogeochemical implications. Rev. Geophys. 52, 603–679. https://doi.org/10.1002/2012RG000417.

Boulton, A., Findlay, S., Marmonier, P., Stanley, E.H., Maurice, Vallet H., 1998. The functional significance of the hyporheic zone in streams and rivers. Ann. Rev. Ecol. Syst. 1998 (29), 59–81. https://doi.org/10.1146/annurev.ecolsys.29.1.59.

Brunner, P., Cook, P.G., Simmons, C.T., 2009. Hydrogeologic controls on disconnection between surface water and groundwater. Water Resour. Res. 45, 1–13. https://doi.org/10.1029/2008WR006953.

Caissie, D., Luce, C.H., 2017. Quantifying streambed advection and conduction heat fluxes. Water Resour. Res. 53 (2), 1595–1624. https://doi.org/10.1002/2016WR019813.

Constantz, J., 2008. Heat as a tracer to determine streambed water exchanges. Water Resour. Res. 44 (4), 1–20. https://doi.org/10.1029/2008WR006996.

Cranswick, R.H., Cook, P.G., Shanafield, M., Lamontagne, S., 2014. The vertical variability of hyporheic fluxes inferred from riverbed temperature data. Water Resour. Res. 50 (5), 3994–4010. https://doi.org/10.1002/2013WR014410.

Cuthbert, M.O., Mackay, R., Durand, V., Aller, M.F., Greswell, R.B., Rivett, M.O., 2010. Impacts of river bed gas on the hydraulic and thermal dynamics of the hyporheic zone. Adv. Water Resour. 33 (11), 1347–1358. https://doi.org/10.1016/j.advwatres.2010.09.014.

Dudley-Southern, M., Binley, A., 2015. Temporal responses of groundwater-surface water exchange to successive storm events. Water Resour. Res. 51 (2), 1112–1126. https://doi.org/10.1002/2014WR016623. arXiv:2014WR016527.

Essaid, H.I., Zamora, C.M., McCarthy, K.A., Vogel, J.R., Wilson, J.T., 2008. Using heat to characterize streambed water flux variability in four stream reaches. J. Environ. Qual. 37 (3), 1010–1023. https://doi.org/10.2134/jeq2006.0448.

Flipo, N., Mouhri, A., Labarthe, B., Biancamaria, S., Rivière, A., Weill, P., 2014. Continental hydrosystem modelling: the concept of nested stream-aquifer interfaces. Hydrol. Earth Syst. Sci. 18 (8), 3121–3149. https://doi.org/10.5194/hess-18-3121-2014.

Greswell, R., Ellis, P., Cuthbert, M., White, R., Durand, V., 2009. The design and application of an inexpensive pressure monitoring system for shallow water level measurement, tensiometry and piezometry. J. Hydrol. 373 (3–4), 416–425. https://doi.org/10.1016/j.jhydrol.2009.05.001.

Hatch, C.E., Fisher, A.T., Revenaugh, J.S., Constantz, J., Ruehl, C., 2006. Quantifying surface water-groundwater interactions using time series analysis of streambed thermal records: method development. Water Resour. Res. 42 (10), 1–14. https://doi.org/10.1029/2005WR004787.

American National Standard for Degrees of Protection Provided by Enclosures (IP Code) (Identical National Adoption). National Electrical Manufacturers Association, 2005.

Kalbus, E., Reinstorf, F., Schirmer, M., 2006. Measuring methods for groundwater-surface water interactions: a review. Hydrol. Earth Syst. Sci. 10, 873–887. https://doi.org/10.5194/hessd-3-1809-2006.

Keery, J., Binley, A., Crook, N., Smith, J.W.N., 2007. Temporal and spatial variability of groundwater-surface water fluxes: development and application of an analytical method using temperature time series. J. Hydrol. 336 (1–2), 1–16. https://doi.org/10.1016/j.jhydrol.2006.12.003.

Krause, S., Hannah, D.M., Fleckenstein, J.H., Heppell, C.M., Kaeser, D., Pickup, R., Pinay, G., Robertson, A.L., Wood, P.J., 2011. Inter-disciplinary perspectives on processes in the hyporheic zone. Ecohydrology 4, 481–499. https://doi.org/10.1002/eco.176.

Loumagne, C., Tallec, G., 2013. L'observation long terme en environnement. Exemple du bassin versant de l'Orgeval, Editions Quae.

Malcolm, I.A., Soulsby, C., Youngson, A.F., Hannah, D.M., 2005. Catchment-scale controls on groundwater-surface water interactions in the hyporheic zone: implications for salmon embryo survival. River Res. Appl. 21 (9), 977–989. https://doi.org/10.1002/rra.861.

Mouhri, A., Flipo, N., Rejiba, F., de Fouquet, C., Bodet, L., Kurtulus, B., Tallec, G., Durand, V., Jost, A., Ansart, P., Goblet, P., 2013. Designing a multi-scale sampling system of stream-aquifer interfaces in a sedimentary basin. J. Hydrol. 504, 194–206. https://doi.org/10.1016/j.jhydrol.2013.09.036.

R Core Team, 2013. R: A Language and Environment for Statistical Computing. R Foundation for Statistical Computing; Vienna, Austria.http://www.R-project.org/.

Rivière, A., Gonçalvès, J., Jost, A., Font, M., 2014. Experimental and numerical assessment of transient stream-aquifer exchange during disconnection. J. Hydrol. 517, 574–583. https://doi.org/10.1016/j.jhydrol.2014.05.040.

Rosenberry, D.O., 2008. A seepage meter designed for use in flowing water. J. Hydrol. 359 (1–2), 118–130. https://doi.org/10.1016/j.jhydrol.2008.06.029.

Rosenberry, D.O., LaBaugh, J.W., 2008. Field techniques for estimating water fluxes between surface water and ground water (Technical Report). U.S. Geological Survey.

Rosenberry, D.O., Sheibley, R.W., Cox, S.E., Simonds, F.W., Naftz, D.L., 2013. Temporal variability of exchange between groundwater and surface water based on high-frequency direct measurements of seepage at the sediment-water interface. Water Resour. Res. 49 (5), 2975–2986. https://doi.org/10.1002/wrcr.20198.

Schmadel, N.M., Ward, A.S., Lowry, C.S., Malzone, J.M., 2016. Hyporheic exchange controlled by dynamic hydrologic boundary conditions. Geophys. Res. Lett. 43, 4408–4417. https://doi.org/10.1002/2016GL068286.

Solder, J.E., Gilmore, T.E., Genereux, D.P., Kip, Solomon D., 2016. A tube seepage meter for in situ measurement of seepage rate and groundwater sampling. Groundwater 54 (1), 588–595. https://doi.org/10.1111/gwat.12388.

Sophocleous, M., 2002. Interactions between groundwater and surface water: the state of the science. Hydrogeol. J. 10, 52–67. https://doi.org/10.1007/s10040-001-0170-8.

Stanford, J., Ward, J., 1988. The hyporheic habitat of river ecosystems. Nature 335, 64–66. https://doi.org/10.1038/335064a0.

Strahler, A.N., 1952. Hypsometric (area-altitude) analysis of erosional topography. Geol. Soc. Am. Bull. 63 (11), 1117–1142. https://doi.org/10.1130/0016-7606(1952) 63.

Wickert, A.D., 2014. The ALog: inexpensive, open-source, automated data collection in the field. Emerg. Technol. 95 (2), 166–176. https://doi.org/10.1890/0012-9623-95.2.68.

Xie, Y., Cook, P.G., Shanafield, M., Simmons, C.T., Zheng, C., 2016. Uncertainty of natural tracer methods for quantifying river-aquifer interaction in a large river. J. Hydrol. 535, 135–147. https://doi.org/10.1016/j.jhydrol.2016.01.071.